

Supporting Information

Enhancing performances of organic photovoltaics with incorporating small molecule stereoisomers as the third component

Yu-Wei Su^a, Chung-Hao Chen^b, Bing-Huang Jiang^c, Han-Yi Huang^a, Tzu-Ching Lu^b, Bin Chang^b,
Chih-Ping Chen^{c*}, Kung-Hwa Wei^{b*}

^a Department of Molecular Science and Engineering, Institute of Organic and Polymeric Materials,
National Taipei University of Technology, Taipei 106344, Taiwan

^b Department of Materials Science and Engineering, National Yang Ming Chiao Tung University,
Hsinchu 30010, Taiwan

^c Department of Materials Engineering, Ming Chi University of Technology, New Taipei City
243303, Taiwan

*Corresponding authors

Chih-Ping Chen: cpchen@mail.mcut.edu.tw

Kung-Hwa Wei: khwei@nycu.edu.tw

Material synthesis

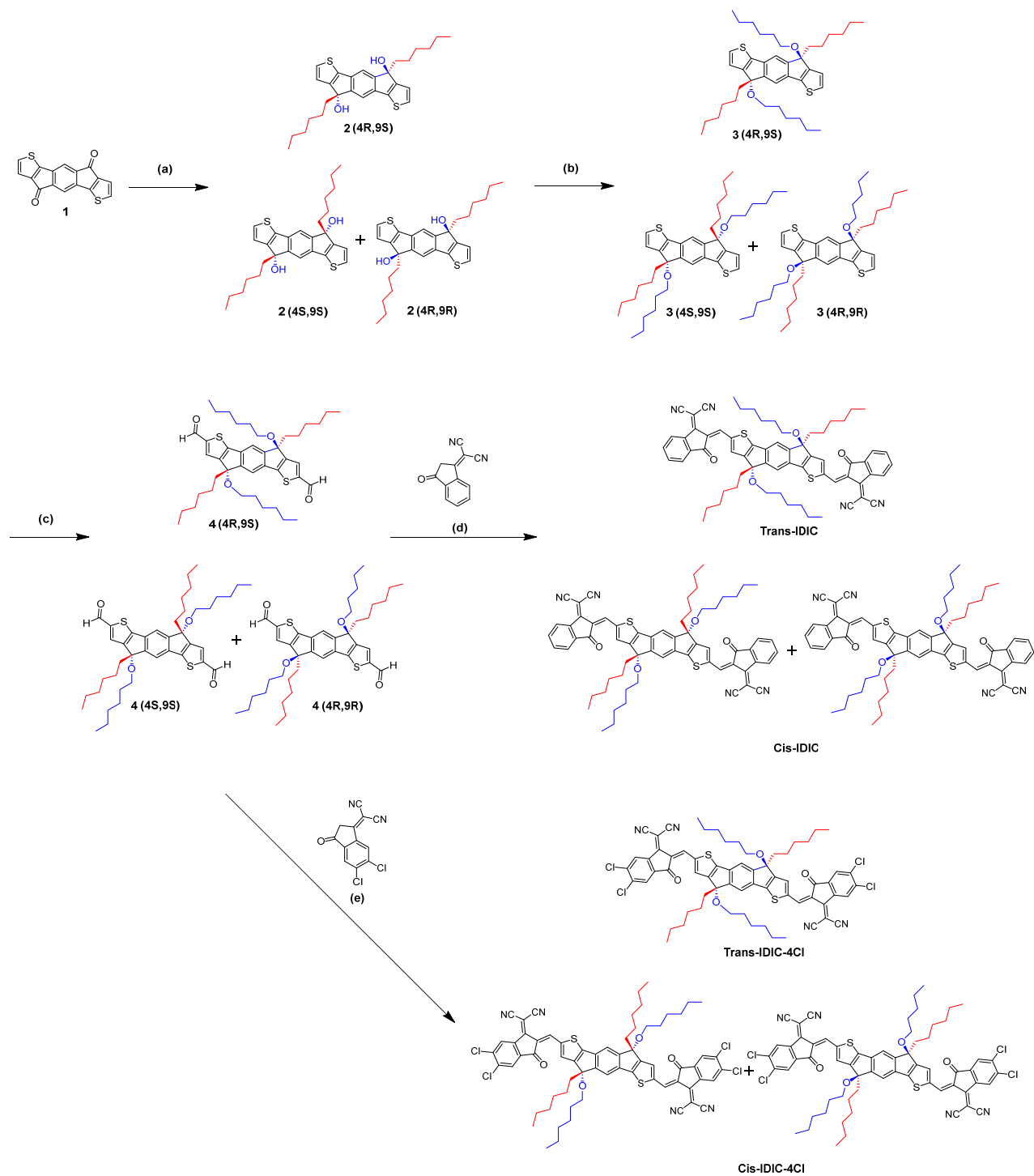


Fig. S1 Syntheses procedures of *cis*-ID-OR, *cis*-ID-OR-4Cl, *trans*-ID-OR and *trans*-ID-OR-4Cl.

1. General product 4,9-dihexyl-4,9-dihydro-s-indaceno[1,2-b:5,6-b']dithiophene -4,9-diol (Compound 2).

To a suspension of magnesium (2.45 g, 102 mmol) and iodine (25 mg, 0.1 mmol) in dry THF (40 mL) was added 1-bromohexane (11.22 g, 68 mmol) slowly under argon, and then the mixture was refluxed for 1 h. The prepared hexyl-1-magnesium bromide (2.55 M, 40mL, 102 mmol) was added to a solution of compound 1 (2 g, 6.8 mmol) dissolving in THF (20 mL) at room temperature under argon. The mixture was refluxed for 12 h and then allowed to cool to room temperature. The aqueous phase was extracted three times with dichloromethane. The organic phase was dried (MgSO₄) and concentrated using a rotary evaporator. The residue was purified by silica gel chromatography using hexanes to DCM/hexanes (1:10) as eluent to give low polarity compound [**Compound 2 (4R,9S)**] first and then the high polarity compound [**Compound 2 (4R,9R)/ Compound 2 (4S,9S)**], based on their difference in polarity.

(4R,9S)-4,9-dihexyl-4,9-dihydro-s-indaceno[1,2-b:5,6-b']dithiophene-4,9-diol [**Compound 2 (4R,9S)**] (1.25 g, 40%)¹H NMR (300 MHz, CDCl₃) δ (ppm): 7.34 (s, 2 H), 7.25 (d, J = 8.0 Hz, 2 H), 7.07 (d, J = 8.0 Hz, 2 H), 2.16 (m, 2 H), 1.97 (m, 2 H), 1.60 (s, 2 H), 1.16 (m, 16 H), 0.88 (t, J = 6.8 Hz, 6 H).

(4R,9R)-4,9-dihexyl-4,9-dihydro-s-indaceno[1,2-b:5,6-b']dithiophene-4,9-diol / (4S,9S)-4,9-dihexyl-4,9-dihydro-s-indaceno[1,2-b:5,6-b']dithiophene-4,9-diol [**Compound 2 (4R,9R)/Compound 2 (4S,9S)**] (1.29 g, 41%). ¹H NMR (300 MHz, CDCl₃) δ (ppm): 7.25 (s, 2 H), 7.20 (d, J = 8.0 Hz, 2 H), 7.01 (d, J = 8.0 Hz, 2 H), 2.43 (s, 2 H), 2.11 (m, 2 H), 1.92 (s, 2 H), 1.14 (m, 16 H), 0.80 (t, J = 6.8 Hz, 6 H).

2. General product 4,9-dihexyl-4,9-bis(hexyloxy)-4,9-dihydro-s-indaceno [1,2-b:5,6-b']dithiophene (Compound 3)

A sample of NaH (1.04 g, 60% in mineral oil, 26 mmol) was washed with hexanes and suspended in anhydrous THF (40 mL) at 0 °C. Compound 2 (1.2 g, 2.6 mmol) dissolving in anhydrous DMF (10 mL) was added slowly under argon, and the reaction mixture at room temperature under argon. To

this mixture 1-bromohexane was added dropwise (4.26 g, 26 mmol). The mixture was heated at 120 °C for 12 h and then allowed to cool to room temperature. The aqueous phase was extracted three times with dichloromethane. The organic phase was dried (MgSO₄) and concentrated using a rotary evaporator. The residue was purified by silica gel chromatography using hexanes as eluent to give the product (4R,9S)-4,9-dihexyl-4,9-bis(hexyloxy)-4,9-dihydro-s-indaceno[1,2-b:5,6-b']dithiophene [**Compound 3 (4R,9S)**] (1.32 g, 80%)¹H NMR (300 MHz, CDCl₃) δ (ppm): 7.27 (d, J = 8.0 Hz, 2 H), 7.25 (s, 2 H), 7.01 (d, J = 6.0 Hz, 2 H), 2.93 (t, J = 8.0 Hz, 4 H), 2.15 (m, 2 H), 1.93 (m, 2 H), 1.40 (m, 4 H), 1.14 (m, 28 H), 0.78 (m, 12 H).

(4R,9R)-4,9-dihexyl-4,9-bis(hexyloxy)-4,9-dihydro-s-indaceno[1,2-b:5,6-b'] dithiophene/(4S,9S)-4,9-dihexyl-4,9-bis(hexyloxy)-4,9-dihydro-s-indaceno [1,2-b:5,6-b']dithiophene [**Compound 3 (4R,9R)/Compound 3 (4S,9S)**] (1.28 g, 79%). ¹H NMR (300 MHz, CDCl₃) δ (ppm): 7.25 (d, J = 8.0 Hz, 2 H), 7.24 (s, 2 H), 7.01 (d, J = 6.0 Hz, 2 H), 2.90 (t, J = 8.0 Hz, 4 H), 2.09 (m, 2 H), 1.88 (m, 2 H), 1.39 (m, 4 H), 1.18 (m, 28 H), 0.81 (m, 12 H).

3. General product 4,9-dihexyl-4,9-bis(hexyloxy)-4,9-dihydro-s-indaceno [1,2-b:5,6-b']dithiophene-2,7-dicarbaldehyde (Compound 4)

To a solution of compound 3 (1.2 g, 1.9 mmol) in THF (60 mL) at -78 °C was added 2.0 M n-butyllithium in hexane (2.85 mL, 5.7 mmol) dropwise slowly under argon. The mixture was stirred at -78 °C for 1 h, and then anhydrous DMF (65.8 mg, 6.0 mmol) was added. The mixture was stirred overnight at room temperature. Brine (50 mL) was added and the mixture and aqueous phase was extracted three times with dichloromethane. The organic phase was dried (MgSO₄) and concentrated using a rotary evaporator. The residue was purified by silica gel chromatography using hexanes to DCM/hexanes (1:5) as eluent to give the product (4R,9S)-4,9-dihexyl-4,9-bis(hexyloxy)-4,9-dihydro-s-indaceno[1,2-b:5,6-b']dithiophene-2,7-dicarbaldehyde [**Compound 4 (4R,9S)**] (1.32 g, 80%)¹H NMR (300 MHz, CDCl₃) δ (ppm): 9.90 (s, 2 H), 7.62 (s, 2 H), 7.46 (s, 2 H), 2.93 (t, J = 8.4 Hz, 4 H), 2.15 (m, 2 H), 1.89 (m, 2 H), 1.42 (m, 4 H), 1.18 (m, 28 H), 0.80 (t, J = 6.8 Hz, 12 H). (4R,9R)-4,9-dihexyl-4,9-bis(hexyloxy)-4,9-dihydro-s-indaceno[1,2-b:5,6-b'] dithiophene-2,7-

dicarbaldehyde/((4S,9S)-4,9-dihexyl-4,9-bis(hexyloxy)-4,9-dihydro-s-indaceno[1,2-b:5,6-b']dithiophene-2,7-dicarbaldehyde [**Compound 4 (4R,9R)/Compound 4 (4S,9S)**] (1.28 g, 79%). ¹H NMR (300 MHz, CDCl₃) δ (ppm): 9.90 (s, 2 H), 7.67 (s, 2 H), 7.47 (s, 2 H), 2.92 (t, J = 8.0 Hz, 4 H), 2.17 (m, 2 H), 1.88 (m, 2 H), 1.41 (m, 4 H), 1.22 (m, 28 H), 0.79 (t, J = 6.8 Hz, 12 H).

4. General product ID-OR

To a solution of compound 4 (250 mg, 0.36 mmol) and 1,1-dicyanomethylene-3-indanone (350 mg, 1.8 mmol) in dry CHCl₃ (50 mL) was added pyridine (1 mL) under argon. The mixture was refluxed for 12 h and then allowed to cool to room temperature. The aqueous phase was extracted three times with CHCl₃. The organic phase was dried (MgSO₄) and concentrated using a rotary evaporator. The residue was purified by silica gel chromatography using hexanes to DCM/hexanes (1:3) as eluent to give the product 2,2'-((2Z,2'Z)-(((4R,9S)-4,9-dihexyl-4,9-bis(hexyloxy)-4,9-dihydro-s-indaceno[1,2-b:5,6-b'] dithiophene-2,7-diyl)bis(methanylylidene))bis(3-oxo-2,3-dihydro-1H-indene-2,1-diylidene)) dimalononitric (*trans*-ID-OR) (255 mg, 68%) ¹H NMR (300 MHz, CDCl₃) δ (ppm): 8.99 (s, 2 H), 8.67 (d, J = 6.8 Hz, 2 H), 7.92 (dd, J₁ = 8.4 Hz, J₂ = 3.2 Hz, 2 H), 7.77 (m, 6 H), 7.60 (s, 2 H), 2.94 (m, 4 H), 2.18 (m, 2 H), 1.96 (m, 2 H), 1.47 (m, 4 H), 1.18 (m, 28 H), 0.78 (m, 12 H). ¹³C NMR (300 MHz, CDCl₃) δ (ppm): 188.25, 160.29, 159.86, 154.26, 153.14, 141.36, 139.95, 138.31, 137.46, 136.89, 135.29, 134.60, 125.38, 123.89, 122.81, 116.78, 114.50, 85.37, 69.75, 64.47, 39.23, 31.92, 31.55, 29.99, 29.69, 29.48, 29.35, 25.64, 24.04, 22.57, 14.06, 14.02.

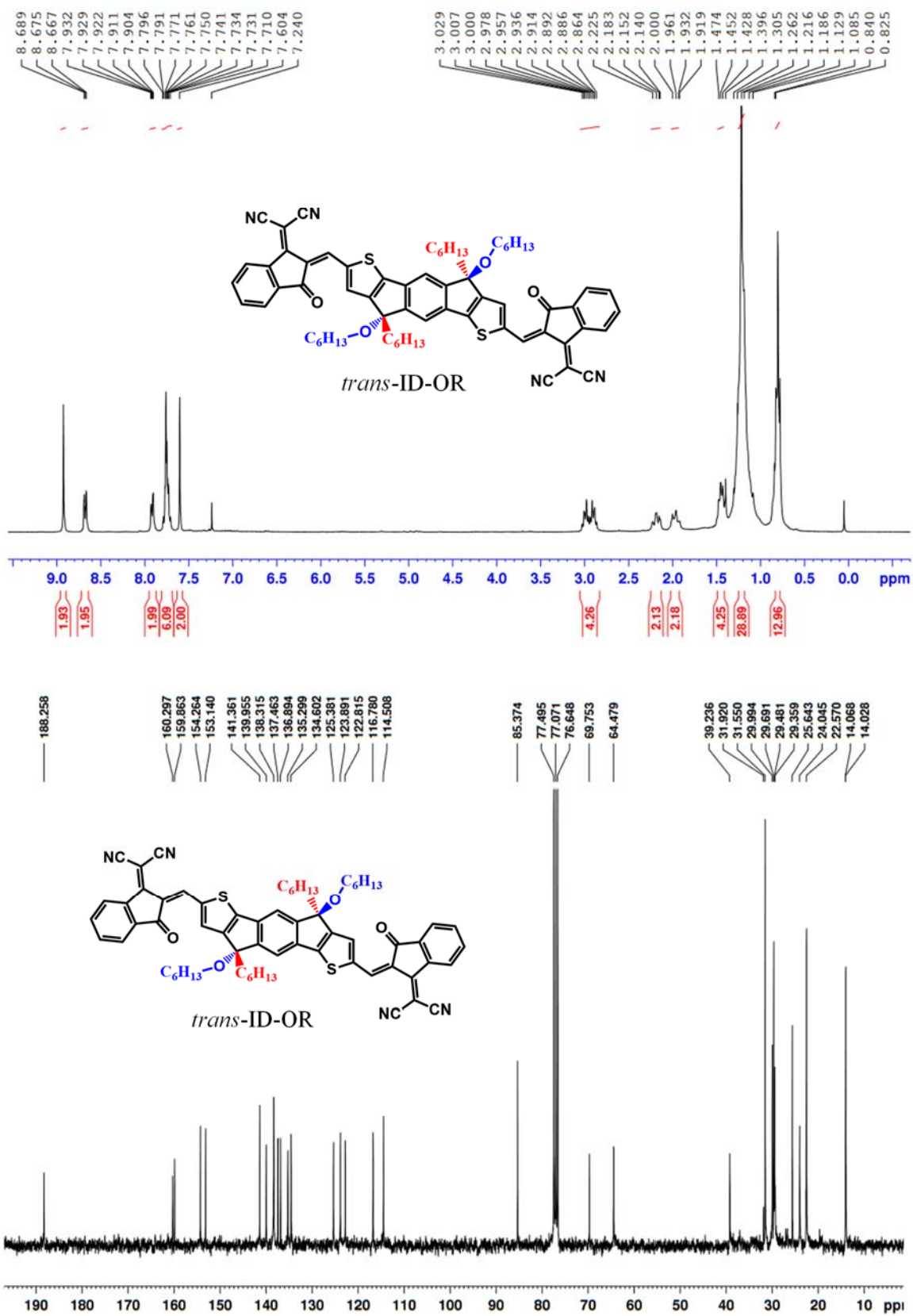


Fig. S2 ¹H NMR and ¹³C NMR spectra of *trans*-ID-OR.

2,2'-((2Z,2'Z)-(((4S,9S)-4,9-dihexyl-4,9-bis(hexyloxy)-4,9-dihydro-s-indaceno [1,2-b:5,6-b']dithiophene-2,7-diyl)bis(methanylylidene))bis(3-oxo-2,3-dihydro-1H-indene-2,1-diylidene))dimalononitrile/2,2'-((2Z,2'Z)-(((4R,9R)-4,9-dihexyl-4,9-bis(hexyloxy)-4,9-dihydro-s-indaceno[1,2-b:5,6-b']dithiophene-2,7-diyl)bis(methanylylidene))bis(3-oxo-2,3-dihydro-1H-indene-2,1-diylidene))dimalononitrile (**cis-ID-OR**) (250 mg, 67%)¹H NMR (300 MHz, CDCl₃) δ (ppm): 8.99 (s, 2 H), 8.70 (d, J = 6.8 Hz, 2 H), 7.95 (dd, J₁ = 8.4 Hz, J₂ = 3.2 Hz, 2 H), 7.77 (m, 6 H), 7.59 (s, 2 H), 2.95 (m, 4 H), 2.14 (m, 2 H), 1.95 (m, 2 H), 1.44 (m, 4 H), 1.18 (m, 28 H), 0.80 (m, 12 H).
¹³C NMR (300 MHz, CDCl₃) δ (ppm): 196.17, 188.30, 160.38, 159.82, 154.24, 153.12, 141.34, 139.97, 138.30, 137.44, 136.91, 135.32, 134.63, 125.40, 123.91, 122.5, 116.75, 114.53, 85.37, 69.75, 64.47, 39.23, 31.54, 29.98, 29.70, 29.47, 25.64, 24.04, 22.56, 14.06, 14.02.

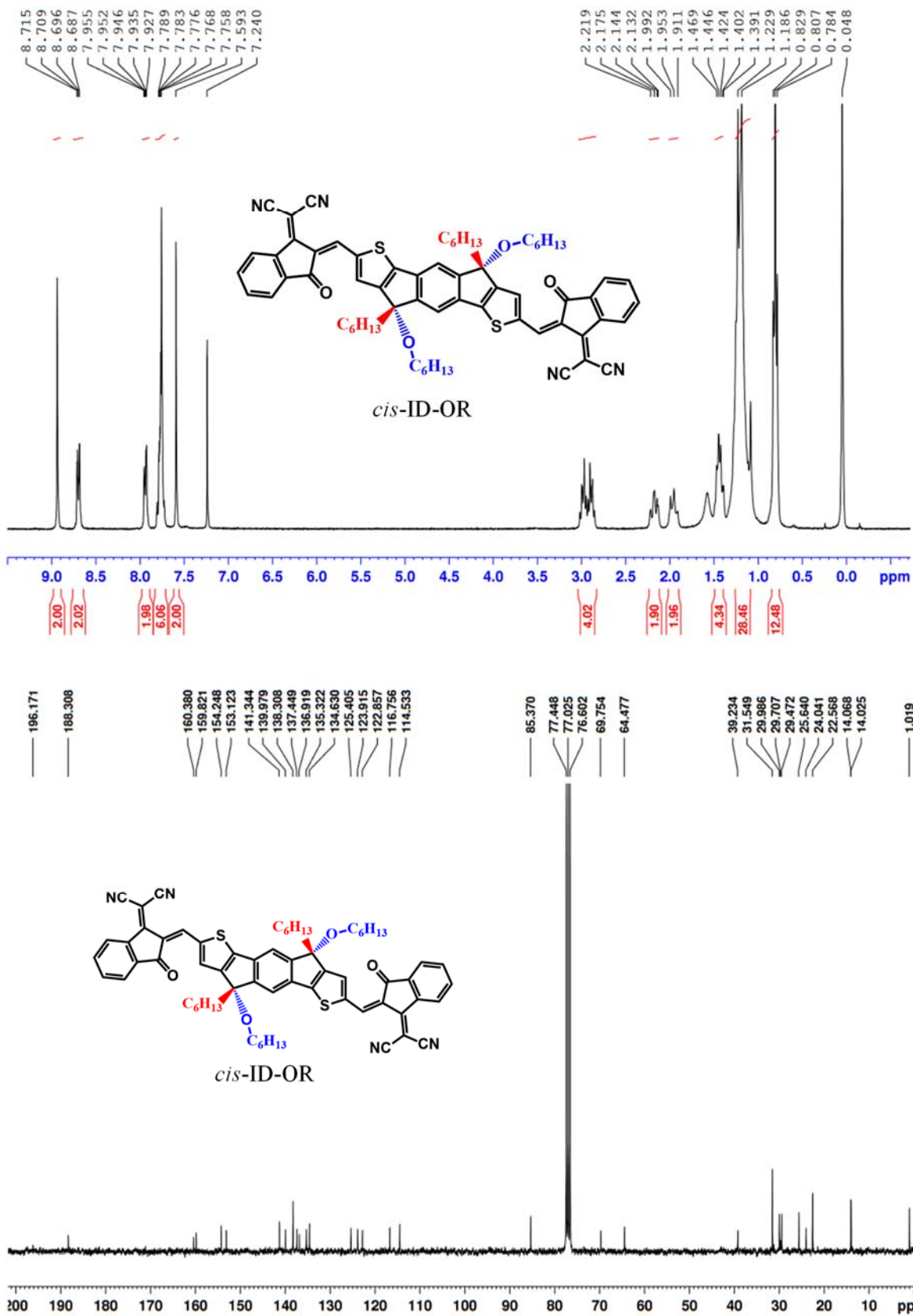


Fig. S3 ¹H NMR and ¹³C NMR spectra of cis-ID-OR.

To a solution of compound 4 (250 mg, 0.36 mmol) and 2-(5,6-dichloro-3-oxo-2,3-dihydro-1H-inden-1-ylidene)malononitrile (473 mg, 1.8 mmol) in dry CHCl₃ (50 mL) was added pyridine (1 mL) under argon. The mixture was refluxed for 8 h and then allowed to cool to room temperature. The aqueous phase was extracted three times with CHCl₃. The organic phase was dried (MgSO₄) and concentrated using a rotary evaporator. The residue was purified by silica gel chromatography using hexanes to DCM/hexanes (1:2) as eluent to give the product 2,2'-((2Z,2'Z)-(((4R,9S)-4,9-dihexyl-4,9-bis(hexyloxy)-4,9-dihydro-s-indaceno[1,2-b:5,6-b']dithiophene-2,7-diyl)bis(methanylylidene))bis(5,6-dichloro-3-oxo-2,3-dihydro-1H-indene-2,1-diylidene))dimalononitrile (**trans-ID-OR-4Cl**) (212 mg, 50%)¹H NMR (300 MHz, CDCl₃) δ (ppm): 8.95 (s, 2 H), 8.77 (s, 2 H), 8.00 (dd, J₁= 8.4 Hz, J₂= 3.2 Hz, 2 H), 7.78 (s, 2 H), 7.62 (m, 2 H), 2.94 (m, 4 H), 2.15 (m, 2 H), 1.98 (m, 2 H), 1.45 (m, 4 H), 1.18 (m, 28 H), 0.80 (m, 12 H). ¹³C NMR (300 MHz, CDCl₃) δ (ppm): 186.01, 160.99, 158.01, 154.55, 153.56, 141.53, 140.00, 139.90, 139.71, 139.09, 138.95, 138.59, 137.53, 136.01, 127.08, 125.36, 121.98, 117.00, 114.12, 114.07, 85.38, 70.47, 64.55, 39.26, 31.55, 31.24, 29.97, 29.70, 29.44, 25.64, 24.05, 22.56, 14.06, 14.02.

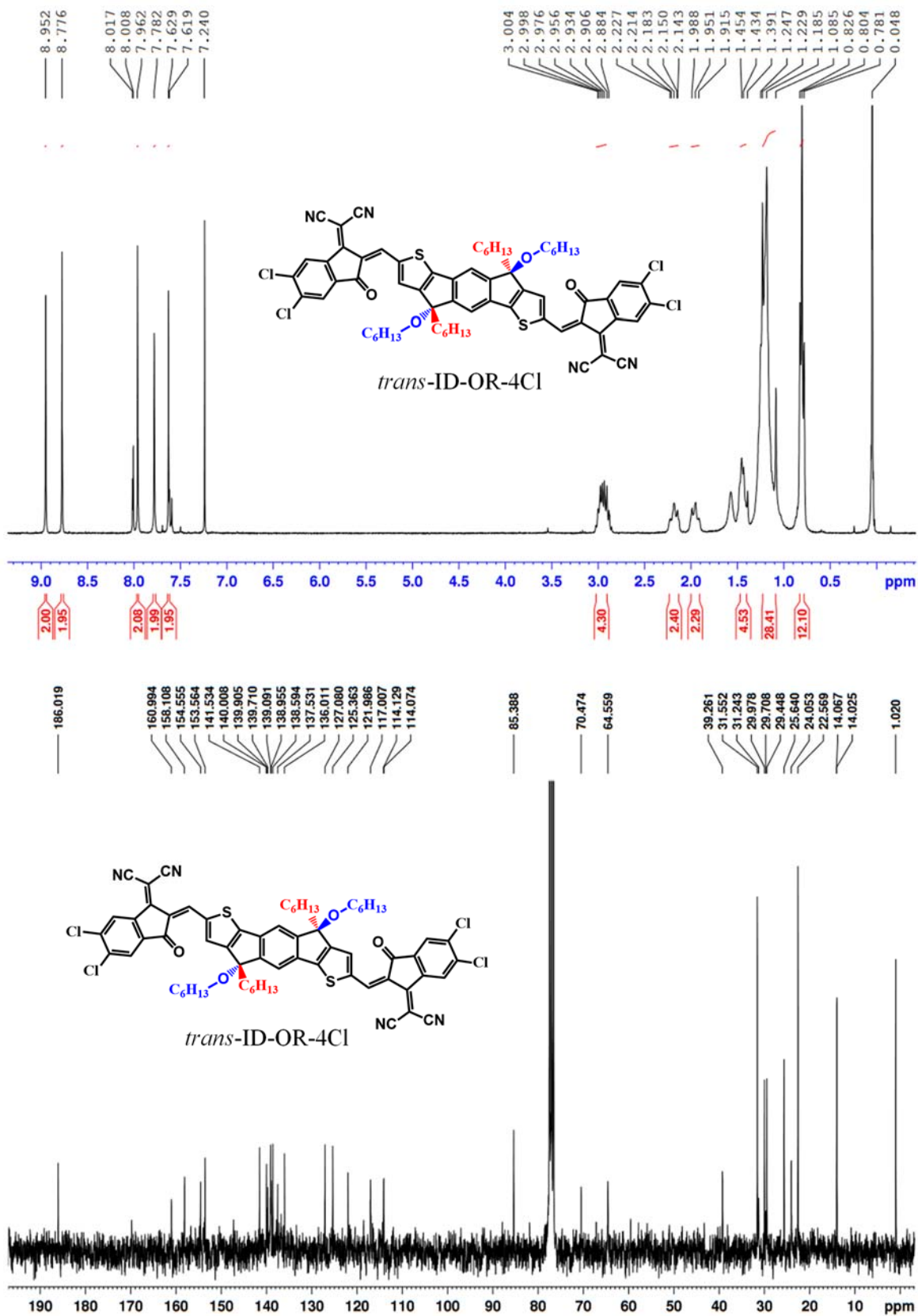


Fig. S4 ¹H NMR and ¹³C NMR spectra of *trans*-ID-OR-4Cl.

2,2'-((2Z,2'Z)-(((4S,9S)-4,9-dihexyl-4,9-bis(hexyloxy)-4,9-dihydro-s-indaceno[1,2-b:5,6-b']dithiophene-2,7-diyl)bis(methanylylidene))bis(5,6-dichloro-3-oxo-2,3-dihydro-1H-indene-2,1-diylidene))dimalononitrile/2,2'-((2Z,2'Z)-(((4R,9R)-4,9-dihexyl -4,9-bis(hexyloxy) -4,9-dihydro-s-indaceno[1,2-b:5,6-b']dithiophene-2,7-diyl) bis(methanylylidene))bis(5,6-dichloro-3-oxo-2,3-dihydro-1H-indene-2,1-diylidene))dimalononitrile (**cis-ID-OR-4Cl**) (200 mg, 47%)¹H NMR (300 MHz, CDCl₃) δ (ppm): 8.94 (s, 2 H), 8.76 (d, 2 H), 7.95 (d, 2 H), 7.78 (s, 2 H), 7.63 (s, 2 H), 2.98 (m, 4 H), 2.17 (m, 2 H), 1.96 (m, 2 H), 1.46 (m, 4 H), 1.22 (m, 28 H), 0.80 (m, 12 H). ¹³C NMR (300 MHz, CDCl₃) δ (ppm): 185.98, 161.03, 158.05, 154.57, 153.57, 141.53, 139.99, 139.70, 139.07, 138.98, 138.58, 137.53, 135.99, 127.06, 125.34, 131.95, 117.01, 114.11, 85.39, 70.46, 64.59, 39.27, 38.14, 31.55, 31.23, 29.98, 29.70, 29.44, 25.64, 24.04, 22.56, 14.06, 14.02

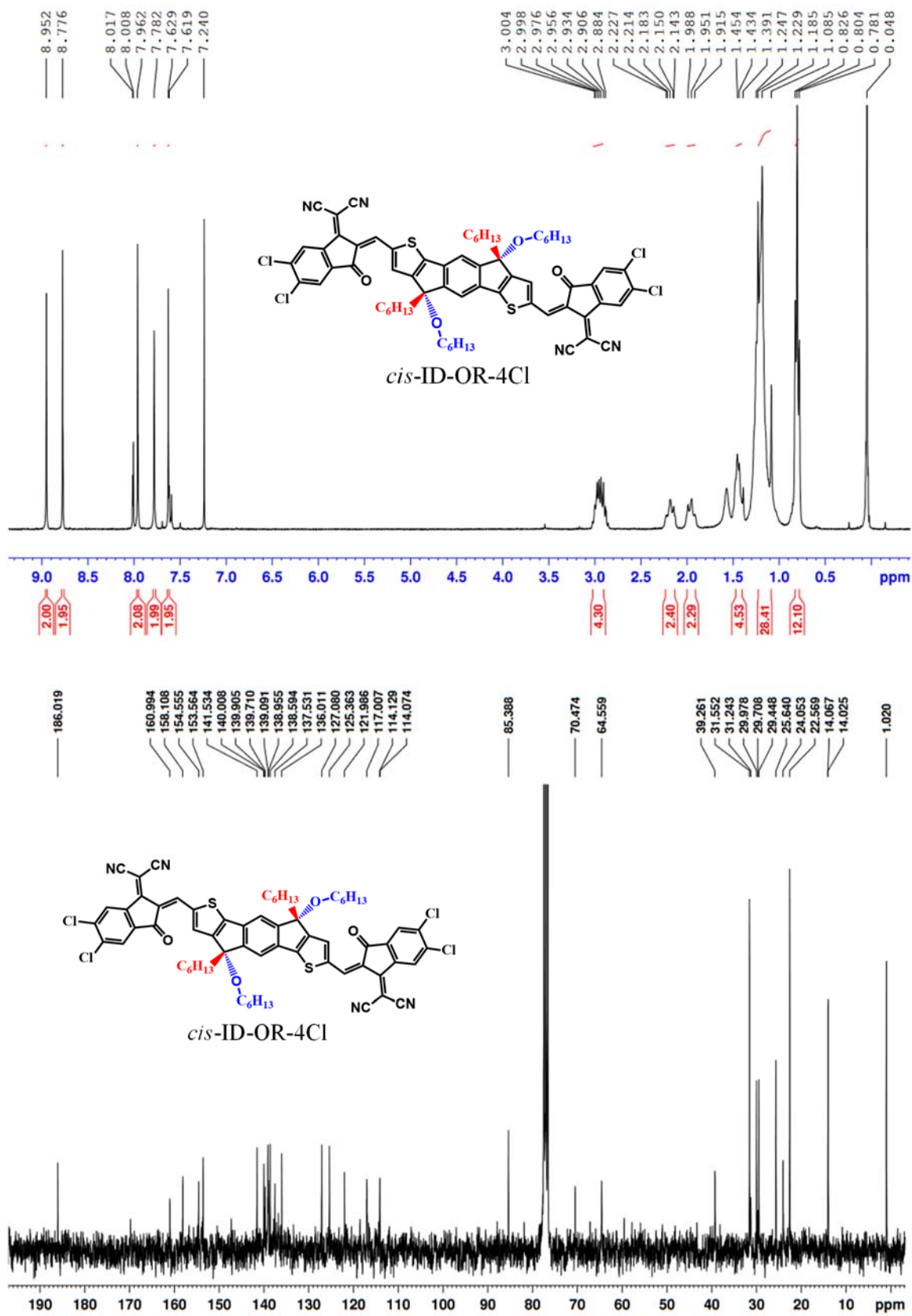


Fig. S5 ¹H NMR and ¹³C NMR spectra of *cis*-ID-OR-4Cl.

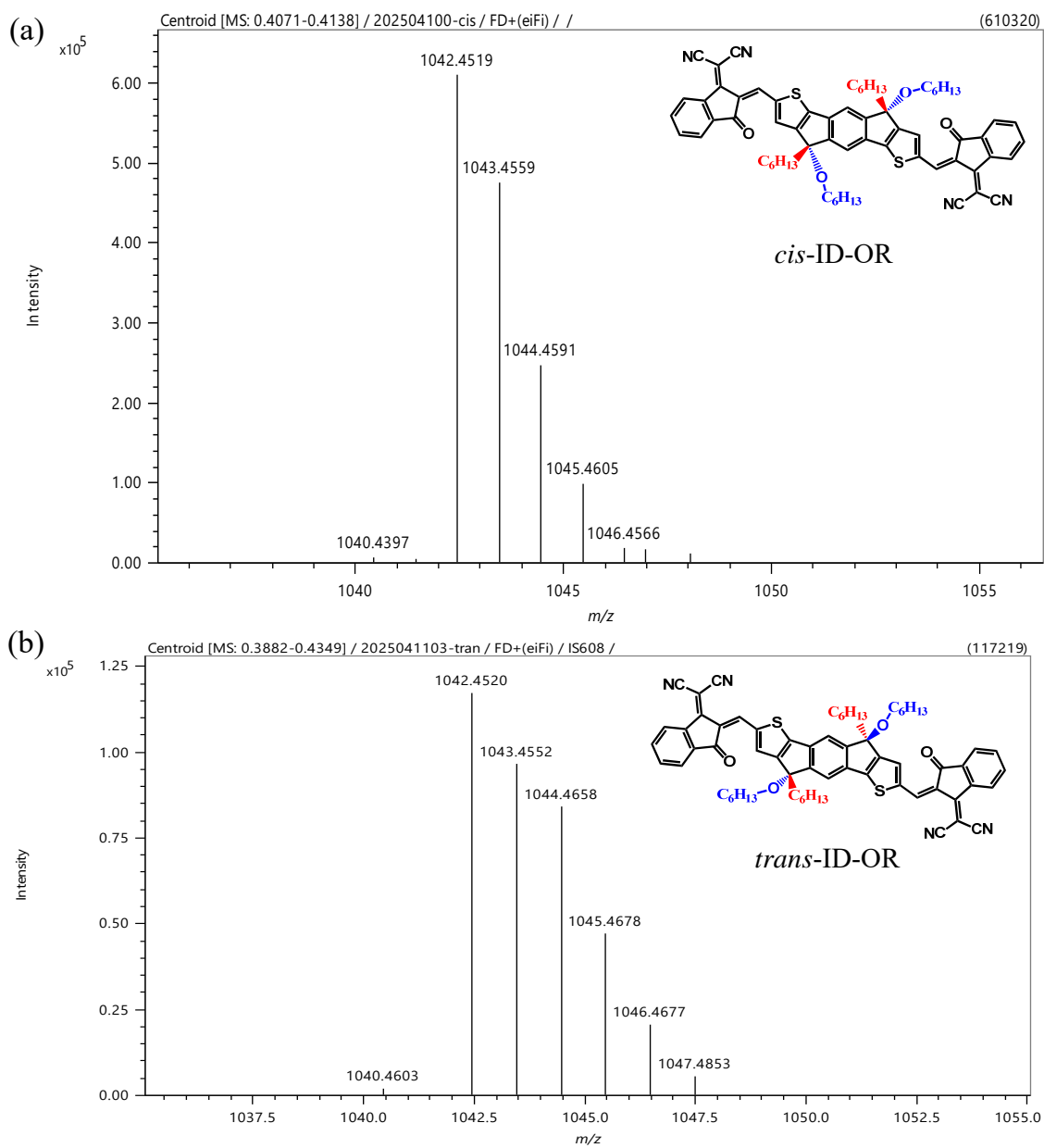


Fig. S6 Mass spectra of (a) *cis*-ID-OR and (b) *trans*-ID-OR. The formulas of both molecules are $C_{66}H_{66}N_4S_2O_4$ ($M_w = 1042$).

Device fabrication

We fabricated OPV devices using an inverted structure of glass/ITO/ZnO/active layer/MoO₃/Ag. The ITO coated glass [Sanyo, Japan (6.4 Ω sq⁻¹)] was cleaned with detergent, ultrasonicated in DI water, acetone and isopropyl alcohol for 20 min, dried in an oven at 120 °C for 30 min. To prepare the sol-gel ZnO precursor solution, the zinc acetate (3.15 g), ethanolamine (0.9 mL), and 2-methoxyethanol (29.1 mL) were mixed and stirred at 25 °C for 3 days. The ITO coated glass substrate was processed by oxygen plasma (Harrick Plasma, PDC-32G) surface treatment lasting for 5 min. The ZnO precursor solution passing through a 0.45-μm filter was spin casted onto the ITO-coated substrate and heated at 160 °C for 10 min in the air to form a ZnO electron transport layer with a thickness of approximately 30 nm. For the binary active layer, the blended solution was prepared via dissolving PM6 (8 mg/ml) and Y6 (8 mg/ml) in chloroform (CF) solvent with 0.75 vol % 1-chloronaphthalene (CN). For the PM6:Y6 based ternary active layer doped stereoisomers small molecule, the precursor solution was prepared via dissolving PM6, Y6 and stereoisomers small molecule (*cis*-ID-OR, *trans*-ID-OR, *cis*-ID-OR-4Cl or *trans*-ID-OR-4Cl) in a weight ratio of 1:1:0.2 in CF (17.6 mg/ml for total concentration) containing 0.75 vol% 1-CN. These solution were stirred overnight in an Ar-filled glove box. Then, it was spin casted onto the glass/ITO/ZnO substrate at room temperature while the thickness of the active layer was optimized by controlling the spin rate and the concentration of the precursor solution. The evaporation equipment with pressures below 10⁻⁶ Torr was used to sequentially deposited a MoO₃ layer (3 nm) and an Ag layer (100 nm) onto the active layer. Among them, the active area was 0.1 cm² which was determined through an overlapping between ITO and Ag. To evaluate the electron and hole trap densities, device structures of ITO/ZnO/active layer/Au and ITO/PEDOT:PSS/active layer/Ag were fabricated, respectively, based on the space-charge limited current (SCLC) model.

Characterization

UV-Vis absorption (Jasco V-650 UV) and photoluminescence (PL) spectra (HORIBA Jobin Yvon) were applied to characterize the optical properties of active layers. Cyclic voltammetry (CV; CH

Instruments 6116E) was used to measure the oxidation and reduction potential of *cis*-ID-OR, *trans*-ID-OR, *cis*-ID-OR-4Cl and *trans*-ID-OR-4Cl to determine the HOMO and LUMO energy level values. The current density–voltage (J–V) and $J_{\text{ph}}-V_{\text{eff}}$ curves of the devices were obtained by using a computer-controlled Keithley 2400 source measurement unit and an Enlitech simulator (AAA Class Solar Simulators) under AM 1.5 illumination ($1000 \text{ W}\cdot\text{m}^{-2}$). The illumination intensity of the EQE was calibrated using a standard Si reference cell cover with a KG-5 filter and matched using an integration system combining a monochromator (Newport 74100), a lock-in amplifier (Stanford Research Systems SR 830), and a chopper to measure the EQE spectra. Grazing-incidence wide-angle X-ray scattering (GIWAXS) analyses was performed at the TLS-23A beamline station in the National Synchrotron Radiation Research Center (NSRRC) Hsinchu Taiwan, using the X-ray wavelength of 1.24 \AA and incident angle of 0.2° . The scattering intensities are reported as intensity versus q [where $q = (4\pi/\lambda) \sin(2\theta/2)$], along with the scattering angles in these patterns; calibration was performed using silver behenate. Surface morphologies of active layers were characterized under ambient conditions using tapping-mode atomic force microscopy (AFM, Bruker Dimension Edge).

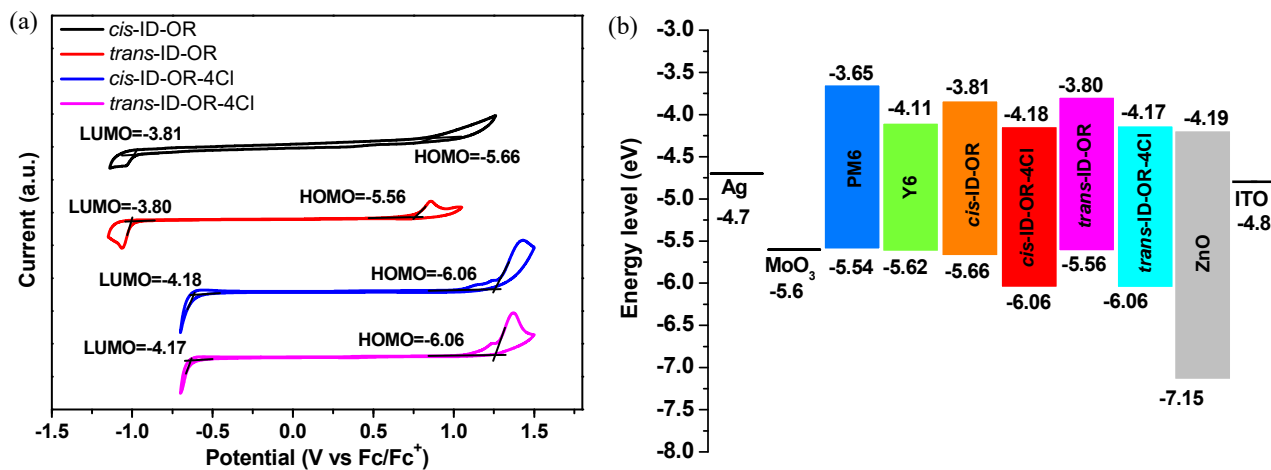


Fig. S7 (a) Cyclic voltammetry curves of the *cis*-ID-OR, *trans*-ID-OR, *cis*-ID-OR-4Cl and *trans*-ID-OR-4Cl. (b) Energy level diagram of each component in the inverted device.

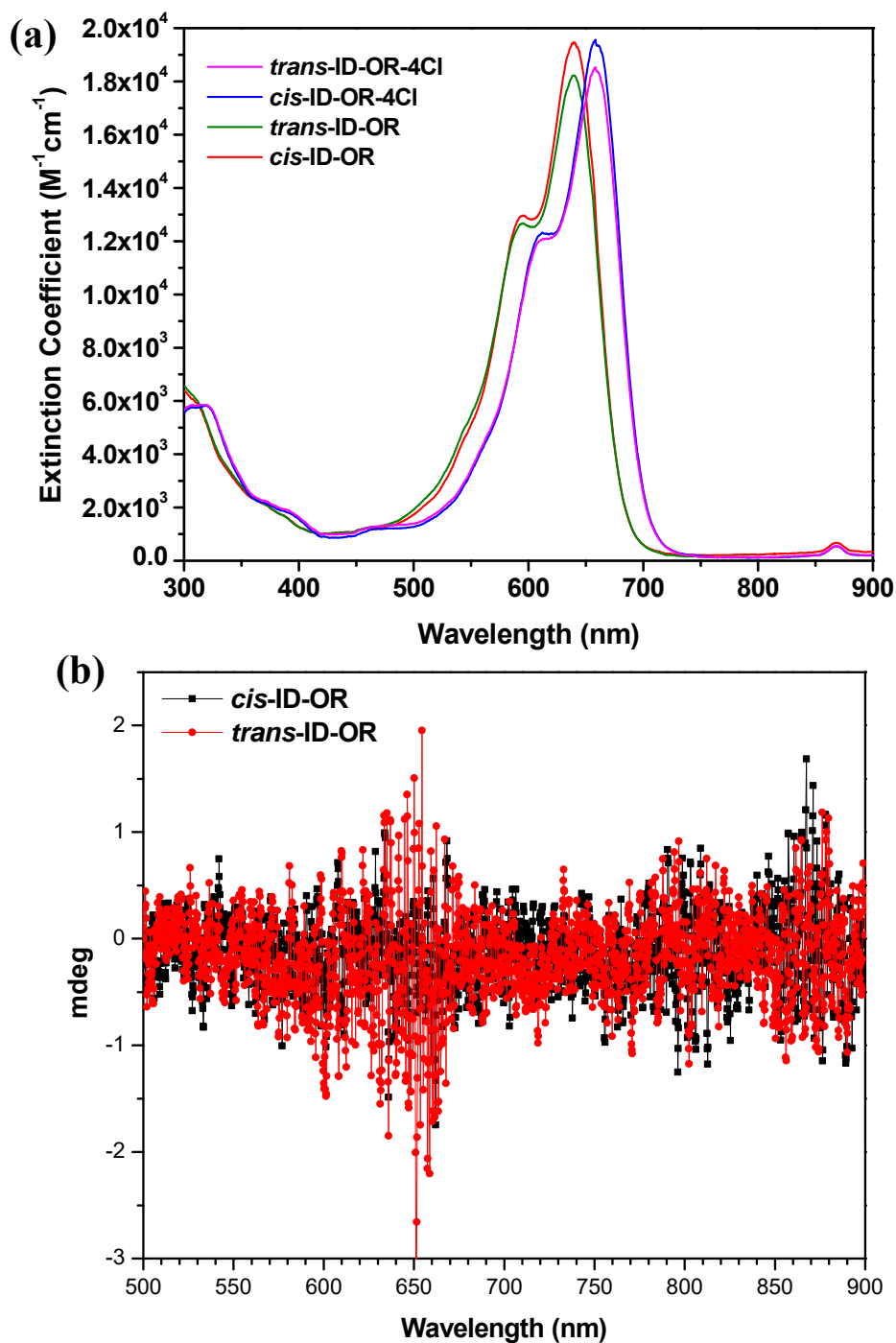


Fig. S8 (a) UV-Vis absorption spectra of *cis*-ID-OR, *trans*-ID-OR, *cis*-ID-OR-4Cl and *trans*-ID-OR-4Cl in chloroform solution. (b) Circular dichroism spectroscopy of *cis*-ID-OR and *trans*-ID-OR.

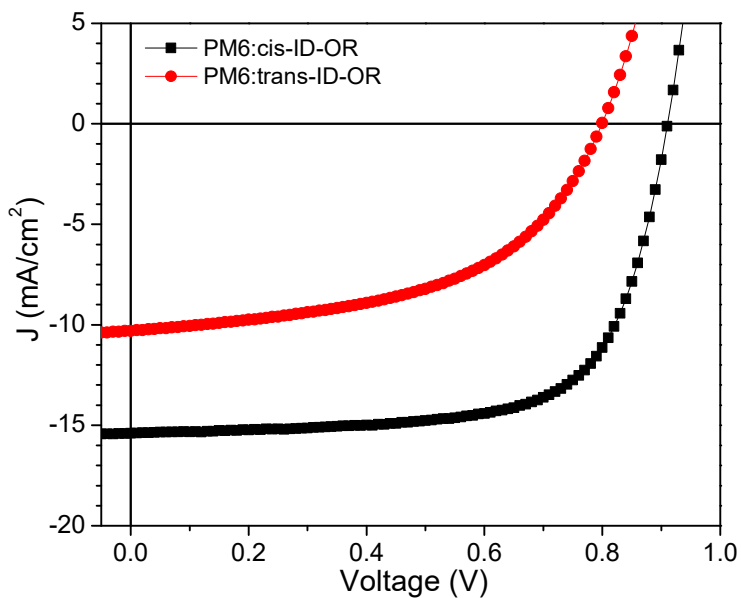


Fig. S9. J–V characteristics of the devices with PM6:*cis*-ID-OR and PM6:*trans*-ID-OR active layers.

Table S1. Photovoltaic parameters of OPV devices incorporating the binary PM6:*cis*-ID-OR and PM6:*trans*-ID-OR active layers.

Ratio 1:1.2 (CN:0.75%) Concentration: 17.6mg/ml	J_{sc} (mA)	V_{oc} (V)	FF (%)	PCE (%)	Best PCE(%)
PM6:<i>cis</i>-ID-OR	14.72 ± 0.53	0.91 ± 0.003	67.3 ± 1.75	9 ± 0.26	9.62
PM6:<i>trans</i>-ID-OR	9.83 ± 0.54	0.79 ± 0.008	51.6 ± 1.37	4 ± 0.19	4.17

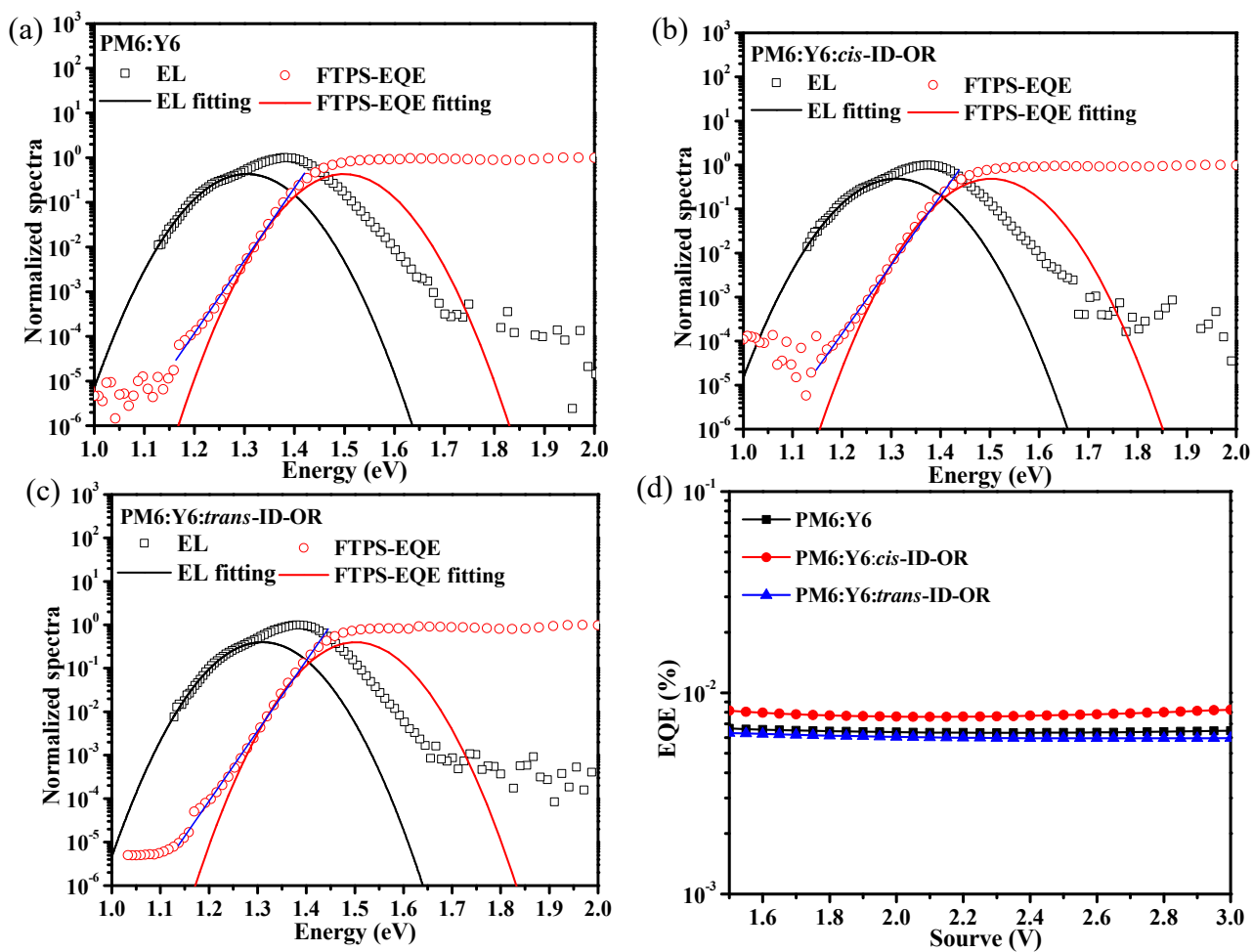


Fig. S10 The normalized EL and FTPS-EQE data points with their fitted curves of (a) PM6:Y6, (b) PM6:Y6:*cis*-ID-OR and (c) PM6:Y6:*trans*-ID-OR. (d) The EQE_{EL} spectra of the binary and ternary OPV.

Table S2. Detailed Energy loss parameters of the binary and ternary OPVs

Blend	E_g [eV]	V_{OC} [V]	V_{loss} [V]	E_{CT} [eV]	ΔE_{CT} [eV]	ΔE_{rad} [V]	$\Delta E_{non-rad}$ [V]	EQE_{EL}
PM6:Y6	1.448	0.88	0.568	1.402	0.046	0.274	0.248	6.38×10^{-5}
PM6:Y6: <i>cis</i> -ID-OR	1.444	0.89	0.554	1.407	0.037	0.274	0.243	7.81×10^{-5}
PM6:Y6: <i>trans</i> -ID-OR	1.449	0.88	0.569	1.406	0.043	0.276	0.250	5.96×10^{-5}

Both *cis*-ID-OR and *trans*-ID-OR have relatively higher LUMO levels than Y6, which promote the enhancement of the charge transfer energy (E_{CT}) in the ternary blend. This can further suppress the loss of ΔE_{CT} ($\Delta E_{CT} = E_g - E_{CT}$). Incorporating *cis*-ID-OR in the ternary blend active layer exhibits the lowest $\Delta E_{non-rad}$, which may be attributed to its fine-tuned molecular packing in the blend film, obtaining the largest CCL of the (010) π - π stacking plane in the ternary blend with Y6. This suppresses defect-induced charge recombination, which aligns with the improvement in trap-assisted recombination observed in the PM6:Y6:*cis*-ID-OR ternary blend. When *trans*-ID-OR is blended in PM6:Y6, the CCL was decreased and a significant decrease in diffraction signal of the *trans*-ID-OR:Y6 binary. This phenomenon indicates disorder in the *trans*-ID-OR acceptor blend, corresponding to a larger $\Delta E_{non-rad}$ and more severe trap-assisted recombination.

Table S3. Optoelectronic parameters calculated from $J_{ph}-V_{eff}$ curves.

Active layer configuration	J_{sat} (mA cm ⁻²)	P(E,T) (%)	G_{max} (m ⁻³ s ⁻¹)	n
PM6:Y6	26.35	92.6	1.65×10^{28}	1.49
PM6:Y6: <i>cis</i> -ID-OR	26.59	96.1	1.66×10^{28}	1.45
PM6:Y6: <i>trans</i> -ID-OR	26.23	95.2	1.64×10^{28}	1.51
PM6:Y6: <i>cis</i> -ID-OR-4Cl	25.79	93.6	1.61×10^{28}	1.48
PM6:Y6: <i>trans</i> -ID-OR-4Cl	25.72	94.5	1.61×10^{28}	1.45

$$J_{ph} = J_{light} - J_{dark} \quad \text{eq (1)}$$

$$V_{eff} = V_0 - V_a \quad \text{eq (2)}$$

$$J_{sat} = qG_{max} L \quad \text{eq (3)}$$

$$J_{ph} = qG_{max} P(E,T)L \quad \text{eq (4)}$$

$$V_{oc} \propto \frac{nkT}{q} \ln(P_{light}) \quad \text{eq (5)}$$

The J_{ph} , J_{light} , J_{dark} and J_{sat} , are the photo, light, dark and saturation current densities, respectively; V_a is the applied voltage; V_0 is the voltage at $J_{ph} = 0$; q is the elementary charge; and L is the thickness of the blend film. The J_{ph} is determined by subtracting dark from light current densities at short circuit condition. The values of J_{ph} of the devices increased significantly at low V_{eff} (< 0.1 V) and became saturated after 0.2 V. Table S3 summarizes the parameters of J_{sat} , $P(E, T)$ and G_{max} calculated from the $J_{ph}-V_{eff}$ curves. The value of J_{sat} related to the absorbed incident photon flux was obtained from J_{ph} under a condition of V_{eff} at 2.5 V, and then the obtained J_{sat} was applied in eq (3) to determine the G_{max} value. The $P(E, T)$ can be calculated from the eq (4) or by the ratio of J_{ph}/J_{sat} . The exciton dissociation probability in blend films was related to the size of their phase-segregated domains, significantly affecting the fill factor of the corresponding devices.

For evaluating the degree of charge carrier recombination relative to trap-assisted recombination, the fitted n value can be obtained by eq (5), where k is the Boltzmann constant, T is the absolute temperature in K, and q is the elementary charge. The fitted n values could be used to evaluate the degree of charge carrier recombination relative to trap-assisted recombination.

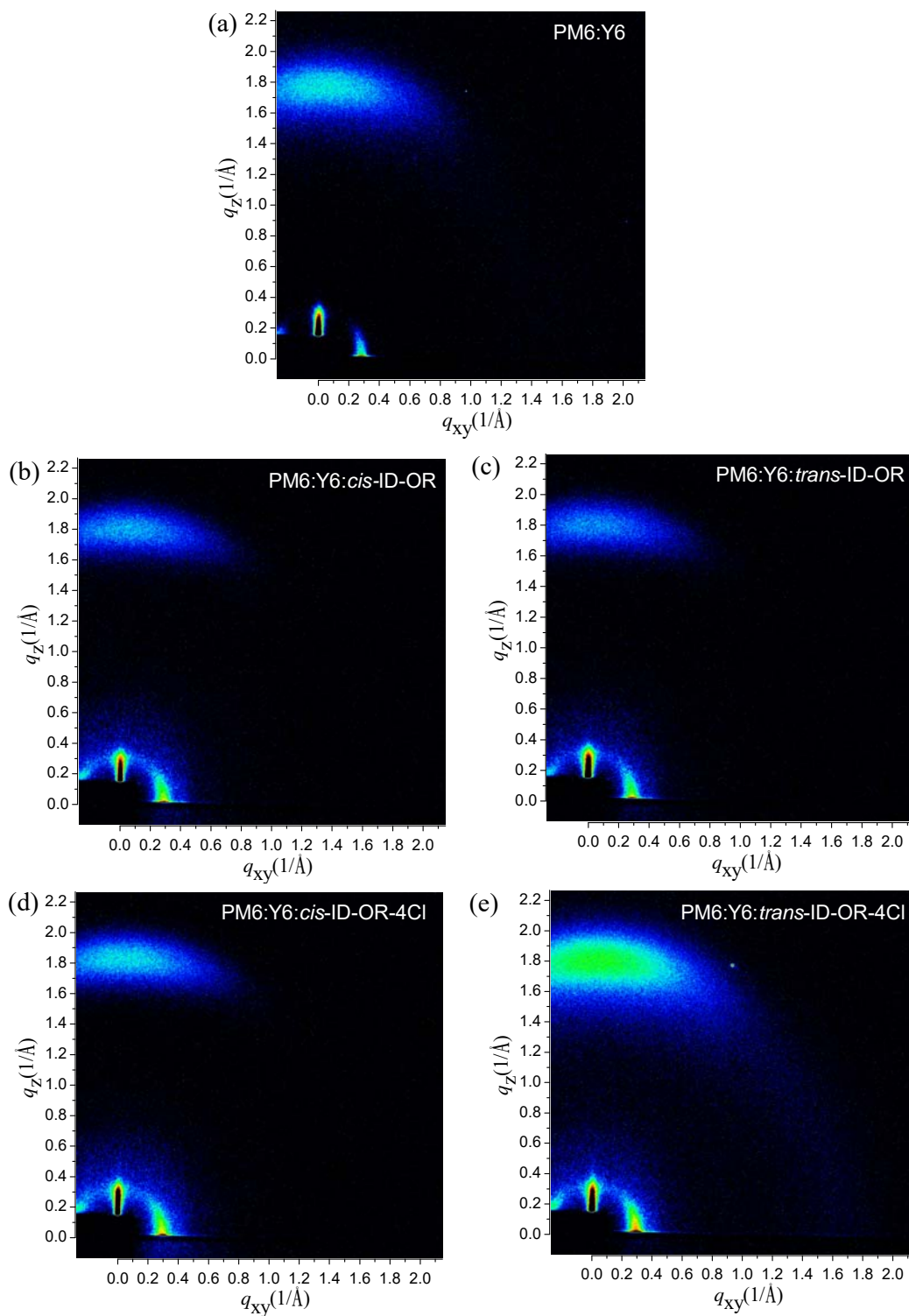


Fig. S11 2-D GIWAXS profiles of (a) PM6:Y6 binary, (b) PM6:Y6:*cis*-ID-OR, (c) PM6:Y6:*trans*-ID-OR, (d) PM6:Y6:*cis*-ID-OR-4Cl, and (e) PM6:Y6:*trans*-ID-OR-4Cl ternary blend films. (PM6:Y6 =1:1 wt ratio, and PM6:Y6:the third component = 1:1:0.2 wt ratio)

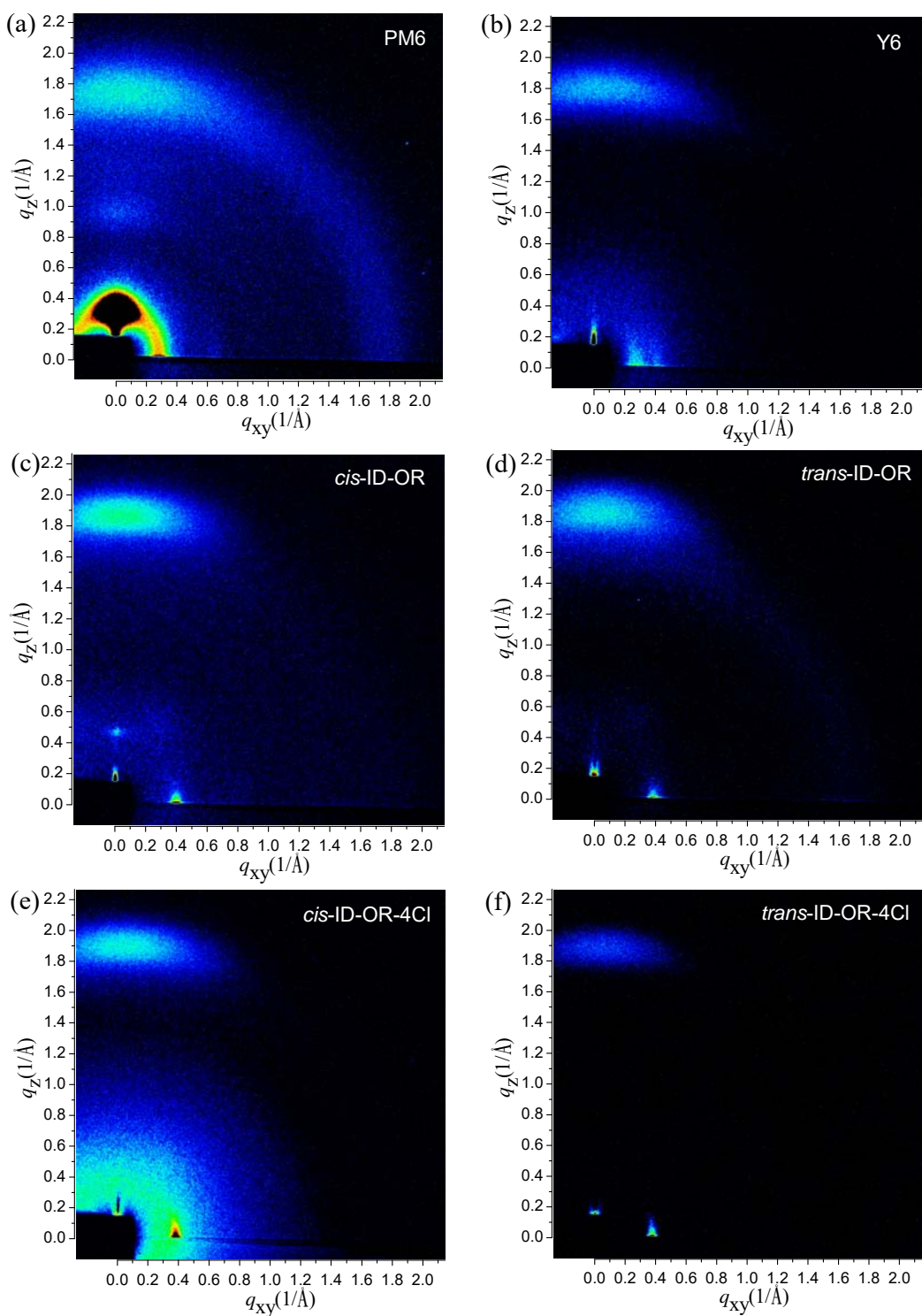


Fig. S12 2-D GIWAXS profiles of pristine (a) PM6, (b) Y6, (c) *cis*-ID-OR, (d) *trans*-ID-OR, (e) *cis*-ID-OR-4Cl, and (f) *trans*-ID-OR-4Cl films.

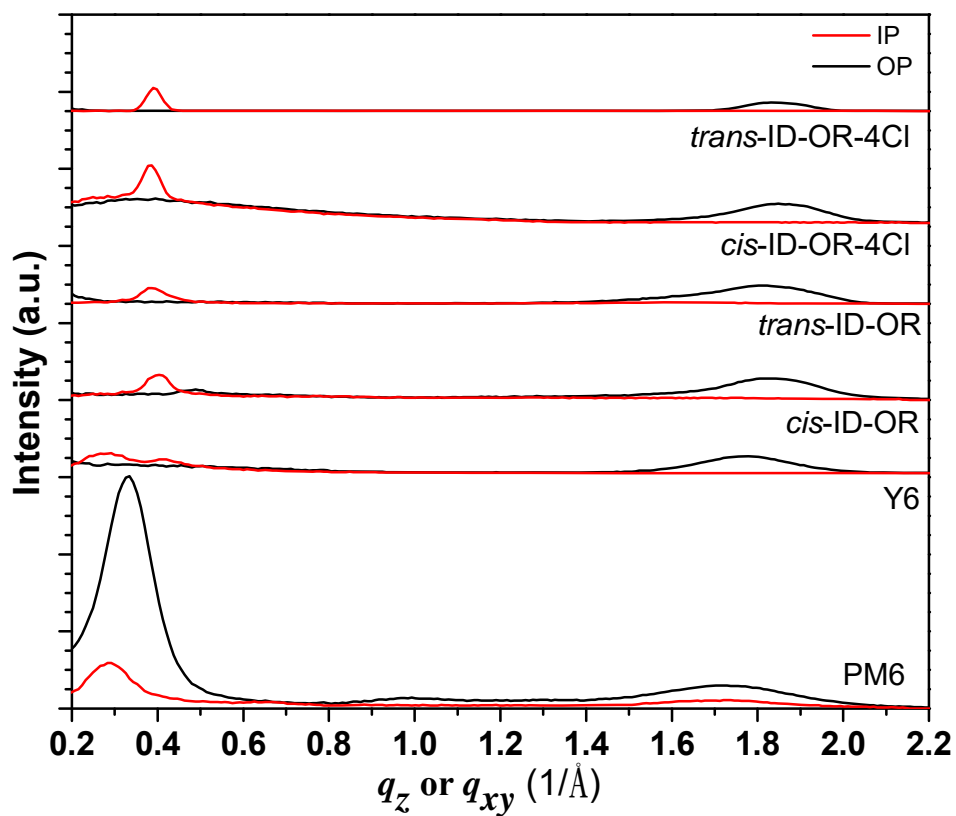


Fig. S13 1-D GIWAXS profiles of pristine PM6, Y6, *cis*-ID-OR, *trans*-ID-OR, *cis*-ID-OR-4Cl, and *trans*-ID-OR-4Cl films.

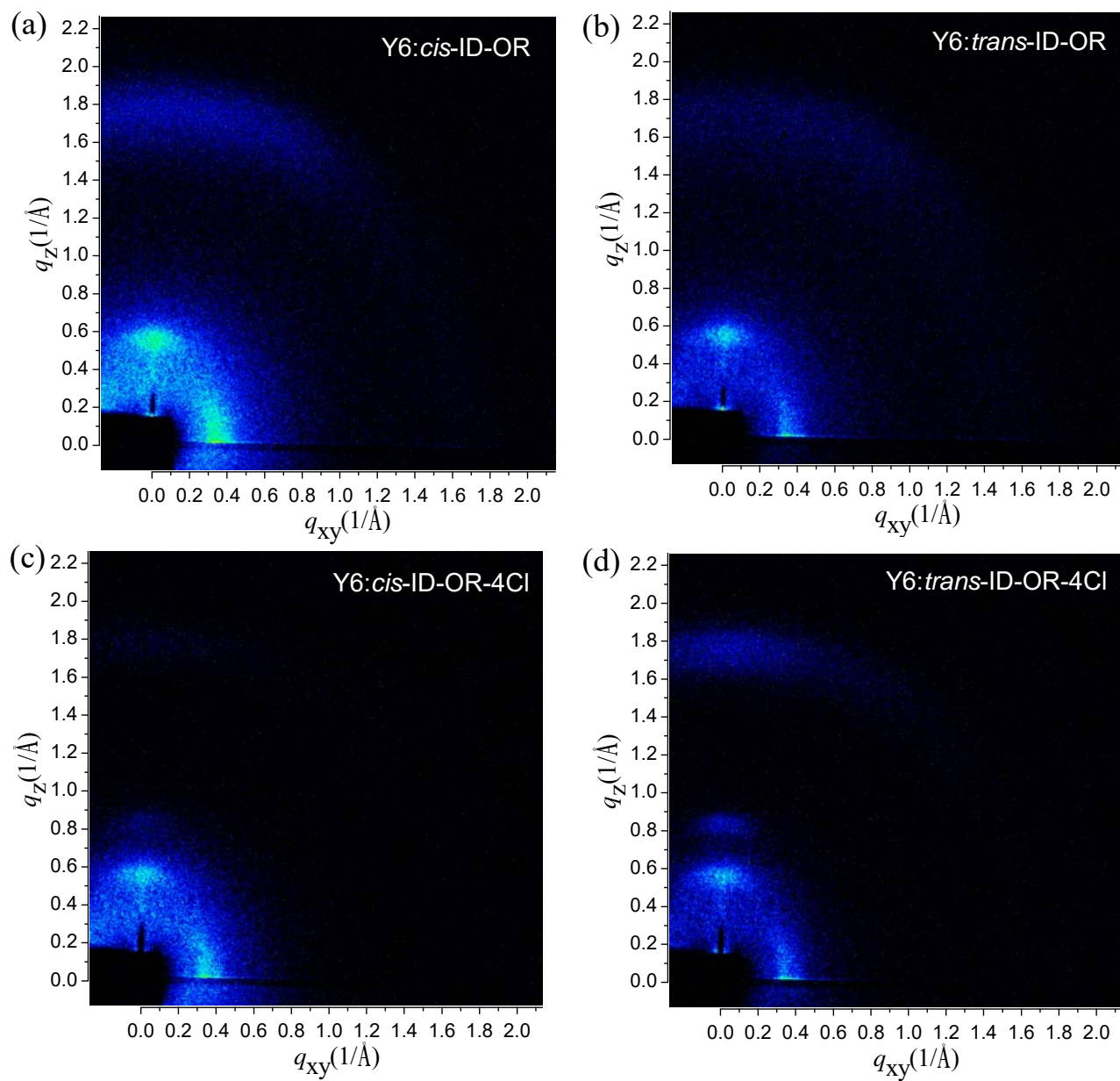


Fig. S14 2-D GIWAXS profiles of (a) Y6:*cis*-ID-OR, (b) Y6:*trans*-ID-OR, (c) Y6:*cis*-ID-OR-4Cl, and (d) Y6:*trans*-ID-OR-4Cl binary blend films.